BIOCHEMISTRY
including biophysical chemistry & molecular biology

Article

pubs.acs.org/biochemistry

ATP-Induced Dimerization of the F_0F_1 ε Subunit from *Bacillus* PS3: A Hydrogen Exchange–Mass Spectrometry Study

Antony D. Rodriguez, Stanley D. Dunn,* and Lars Konermann*

Departments of Chemistry and Biochemistry, The University of Western Ontario, London, Ontario N6A 5B7, Canada

Supporting Information

ABSTRACT: F_0F_1 ATP synthase harnesses a transmembrane electrochemical gradient for the production of ATP. When operated in reverse, this multiprotein complex catalyzes ATP hydrolysis. In bacteria, the ε subunit is involved in regulating this ATPase activity. Also, ε is essential for coupling ATP hydrolysis (or synthesis) to proton translocation. The ε subunit consists of a β sandwich and two C-terminal helices, α1 and α2. The protein can switch from a compact fold to an alternate conformation where α1 and α2 are separated, resulting in an extended structure. ε from the thermophile *Bacillus* PS3 (Tε) binds ATP with high affinity such that this protein may function as an intracellular ATP level sensor. ATP binding to isolated Tε triggers a major conformational transition. Earlier data were interpreted in terms of an ATP + T$\varepsilon_{extended}$ → ATP·T$\varepsilon_{compact}$ transition that may mimic aspects of the regulatory switching within F_0F_1 (Yagi et al. (2007) *Proc. Natl. Acad. Sci. U.S.A., 104*, 11233−11238). In this work, we employ complementary biophysical techniques for examining the ATP-induced conformational switching of isolated Tε. CD spectroscopy confirmed the occurrence of a large-scale conformational transition upon ATP binding, consistent with the formation of stable helical structure. Hydrogen/deuterium exchange (HDX) mass spectrometry revealed that this transition is accompanied by a pronounced stabilization in the vicinity of the ATP-binding pocket. Surprisingly, dramatic stabilization is also seen in the β8−β9 region, which is remote from the site of ATP interaction. Analytical ultracentrifugation uncovered a previously unrecognized feature of Tε: a high propensity to undergo dimerization in the presence of ATP. Comparison with existing crystallography data strongly suggests that the unexpected β8−β9 HDX protection is due to newly formed protein−protein contacts. Hence, ATP binding to isolated Tε proceeds according to 2ATP + 2T$\varepsilon_{extended}$ → (ATP·T$\varepsilon_{compact}$)$_2$. Implications of this dimerization propensity for the possible role of Tε as an antibiotic target are discussed.

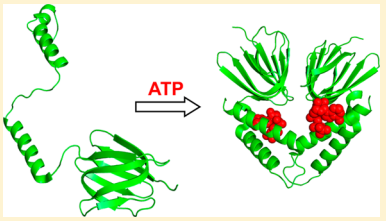

ATP synthase is the molecular machine responsible for the production of adenosine triphosphate from ADP and P_i.[1−3] This multiprotein complex is associated with the plasma membrane of bacteria, the inner mitochondrial membrane, and the thylakoid membrane of chloroplasts.[4] The proton-motive force (PMF)[5] that drives ATP synthesis is established by transmembrane proton translocation during respiration or photosynthesis. The overall architecture of ATP synthase in bacteria, mitochondria, and chloroplasts is similar, with a membrane-embedded F_0 portion and a cytosolic F_1 portion. F_0 from bacteria exhibits the subunit stoichiometry ab_2c_n (with n = 10 for *Escherichia coli*), and bacterial F_1 has the composition $(\alpha\beta)_3\gamma\delta\varepsilon$ (Figure 1A). Transmembrane proton flow causes rotation of the $c_n\gamma\varepsilon$ subcomplex. γ extends deep into the catalytic head, and its rotation triggers a series of conformational changes in $(\alpha\beta)_3$ that are coupled to the synthesis and release of three ATP molecules per revolution.[6]

The conversion of electrochemical energy to mechanical energy, and ultimately to chemical energy, represents the normal function of ATP synthase. However, the enzyme is also capable of operating in reverse.[7] This ATPase activity can help the cell cope with a drop in PMF and is essential during fermentative growth. Under such conditions, ATP hydrolysis keeps the membrane energized, thereby maintaining the viability of processes such as ion transport and flagellar motion.[8] This hydrolytic activity of F_0F_1 must be tightly regulated because a depletion of the cellular ATP pool can have catastrophic consequences for the cell. One regulatory mechanism in bacteria, plants, and mitochondria involves binding of MgADP (without P_i) to catalytic sites on $(\alpha\beta)_3$, resulting in deactivation of the complex.[7,9−11]

A second regulatory mechanism that is found exclusively in bacterial F_0F_1 involves the ε subunit.[12,13] The role of ε appears to be 2-fold. One one hand, during ATP synthesis, ε is required for effective coupling.[14,15] On the other hand, ε represents an inhibitor of F_1-mediated ATP hydrolysis.[9,11,16,17] ε is a ∼15 kDa protein that can adopt at least two different conformations. Studies on isolated ε from *E. coli* (Eε) revealed a compact structure consisting of two domains (Figure 1B).[18,19] The N-terminal part folds into a β sandwich that comprises 10 strands. The C-terminal domain forms a helix−loop−helix motif. Contacts between these helices (α1 and α2) are mediated by interdigitation of Ala residues. Hydrophobic contacts are found at the interface of the two domains. A similar compact structure is seen for the mitochondrial homologue of ε (δ) when it is bound to F_1.[20] Cross-linking[21] and crystallization studies[22,23] provided initial evidence that Eε can also adopt a more

Received: April 17, 2014
Revised: May 26, 2014
Published: May 28, 2014

dx.doi.org/10.1021/bi5004684 | *Biochemistry* 2014, 53, 4072−4080

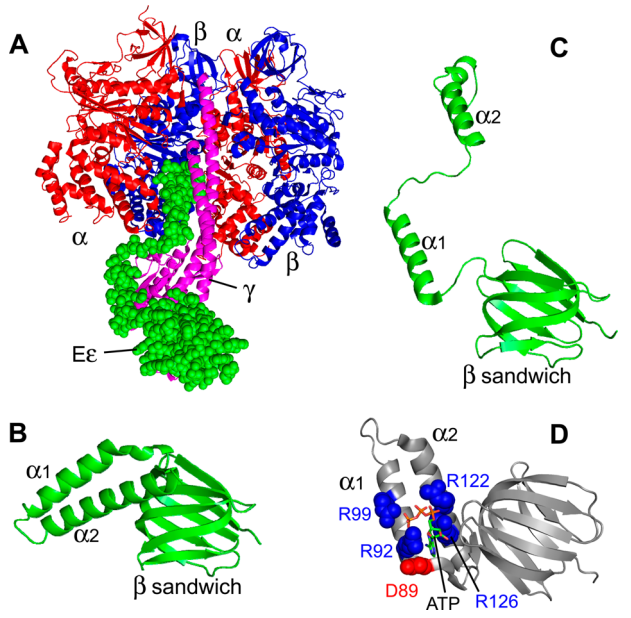

Figure 1. (A) Crystal structure of the *E. coli* F_1 complex with subunits α (red), β (blue), γ (purple), and ε (referred to as Eε from now on; space-filled in green). One $\alpha\beta$ pair facing the observer has been omitted to provide a better view (PDB file 3OAA).[14] (B) Compact state of Eε observed after crystallization of the isolated protein (PDB file 1AQT).[18] (C) Close-up of Eε in the extended conformation within the F_1 complex (from panel A). The orientation of the β sandwich in panels A–C is the same. (D) Crystal structure of ε from *Bacillus* PS3 (referred to as Tε from now on) in the ATP-bound compact state (PDB file 2E5Y).[23] Key residues that interact with the ligand are shown in space-filled representation. The triphosphate group of ATP is depicted in red/orange. Note that the orientations of Eε and Tε in panels B and D are different.

extended structure. This was confirmed by X-ray analysis of *E. coli* F_1, where the helix–loop–helix motif of Eε has opened up such that α2 extends into the catalytic head where it interacts with γ and $(\alpha\beta)_3$ (Figure 1A,C).[14] It has been proposed that the compact state of Eε allows both ATP synthesis and hydrolysis to occur. The extended form may permit rotation in the synthesis direction only, while shutting down ATP hydrolysis.[24] However, recent studies indicate that the mechanism of ε-mediated F_0F_1 inhibition is more complex than envisioned in this simple ratchet model.[3,7,9,14]

The switching state of ε within bacterial F_0F_1 depends on the PMF and on the torque applied to γ.[14] The ε conformation is also affected by the presence of ATP.[25] An ATP-binding site has been identified for ε from the thermophilic bacterium *Bacillus* PS3 (Tε). ATP-bound isolated Tε crystallizes in the compact state (Figure 1D).[23] Other nucleoside triphosphates do not interact with the protein.[26,27] This specificity has led to the suggestion that Tε may serve as an intracellular ATP level sensor.[26,27] Sequence analyses point to I(L)DXXRA as a conserved ATP-binding motif in many bacterial ε subunits.[23] In the case of Tε, this binding motif comprises residues D89 and R92. In addition, R99, R122, and R126 in helices α1 and α2 participate in the formation of a cationic pocket that accommodates the negatively charged triphosphate group of ATP (Figure 1D). The K_d value of the Tε–ATP interaction is in the submicromolar range at room temperature.[28] Much lower affinities of 22[23] and 2 mM[29] have been reported for isolated Eε and for ε from *Bacillus subtilis*, respectively. Considering the wide range of ATP-binding affinities for ε from different bacteria, the functional role of ε–ATP interactions is yet to be fully elucidated.[26] The ε subunit from chloroplasts does not possess an ATP-binding site.[30] It is also known that the mitochondrial homologue of ε is not involved in F_0F_1 inhibition; instead, the protein IF1 acts as inhibitor of ATPase activity in mitochondria.[31] This implies that bacterial ε represents an interesting antibiotic target.[14,32]

Considering the immense complexity of intact F_0F_1, a potential approach to understand the function of ε is via studies at the isolated protein level. Intriguingly, it has been demonstrated that ATP binding to isolated Tε induces major structural changes in the α1–α2 region.[23,27,28] NMR experiments revealed that even truncated α1–α2 can bind ATP, forming a compact helix–loop–helix fold similar to that seen for ATP-bound Tε. Without ATP, truncated α1–α2 is more dynamic, and the two helices are separated from each other, possibly resembling the inhibitory ε conformation seen in the crystal structure of intact F_0F_1 (Figure 1A).[14] Unfortunately, crystallographic data for ATP-free Tε are not available. Nonetheless, the findings of refs 23 and 28 suggest that functionally relevant ATP-induced switching may take place in isolated Tε, offering the opportunity to examine the switching mechanism by various biophysical techniques.

Hydrogen/deuterium exchange (HDX) coupled with mass spectrometry (MS) is a widely used method for probing protein structure, dynamics, and interactions.[33−42] Solvent-exposed backbone N–H sites in unstructured regions exchange rapidly upon exposure to D_2O, with rate constants on the order of 1 s^{-1}.[43] HDX at backbone sites that are involved in α-helices and β-sheets is much slower. Deuteration at these sites is mediated by conformational fluctuations that induce the transient opening of hydrogen bonds, coupled with exposure of N–H sites to the solvent. Thus, HDX in flexible regions proceeds much faster than in rigid segments. Ligand binding usually stabilizes the protein and induces a reduction in HDX rates. The largest changes tend to occur in regions that interact directly with the ligand, although allosteric effects can play a role as well.[44,45]

Here, we employ HDX–MS in conjunction with circular dichroism (CD) spectroscopy and analytical ultracentrifugation (AUC) for studying the ATP-induced conformational switching of isolated Tε. We also examine the behavior of Eε for comparative purposes. ATP binding to Tε results in a highly unusual HDX protection pattern. With the aid of AUC experiments, we demonstrate that this pattern originates from a previously unrecognized propensity of isolated Tε to dimerize in the presence of ATP.

EXPERIMENTAL SECTION

Materials. 3-(*N*-Morpholino)propanesulfonic acid (MOPS) was purchased from Fischer Scientific (Georgetown, ON), and ATP was from MP Biomedicals (Santa Ana, CA). All purification steps were carried out at 4 °C unless it is noted otherwise. Eε was expressed in in *E. coli* strain MM294 from plasmid pES2[46] and purified by fractionation of cell extracts using ammonium sulfate precipitation followed by chromatography using Biogel HTP hydroxyapatite, DEAE-Sepharose, and Sephadex G-75 columns as described previously.[47] Plasmid pTE2 encoding Tε was kindly provided by Prof. Yasuyuki Kato-Yamada (Department of Life Sciences, Rikkyo University, Japan).[48] It was expressed in *E. coli* strain BL21/DE3. Extracts of induced cells were fractionated by ammonium sulfate

dx.doi.org/10.1021/bi5004684 | *Biochemistry* 2014, 53, 4072–4080

precipitation (45−65% of saturation), ion-exchange chromatography at pH 8.0 on DEAE-Sepharose, and size-exclusion chromatography on a Sephadex G-75 column. Two peaks of pure Tε emerged from the G-75 column. Upon subsequent analysis using an Amersham Superdex 200 10/200 GL analytical size-exclusion column run at 25 °C, the first peak eluted with a 260/280 absorbance ratio of 2.77, implying that it contained bound ATP, in agreement with previous findings.[26] Similar analysis of the second peak gave a 260/280 absorbance ratio of 0.54, implying that it did not contain ATP. However, if a sample of the second peak was incubated with a 2-fold molar excess of ATP before application to the column, then the protein eluted with a 260/280 ratio of 2.80, indicating that it was also capable of binding ATP. The experiments in this work were performed with Tε protein from the first peak. ATP-free protein was generated from this stock by overnight dialysis at 20 °C in the presence of 15 U mL^{-1} yeast hexokinase against a solution containing 200 mM glucose as described previously.[26] Hexokinase was subsequently separated from Tε by size-exclusion chromatography on a preparative Sephadex G-75 column.

Hydrogen/Deuterium Exchange Mass Spectrometry. Ligand binding experiments were performed by initially pre-equilibrating 20 μM protein with either 1 mM (Tε) or 10 mM (Eε) ATP/$MgCl_2$ overnight in 25 mM MOPS-KOH (pH 7.0). Exchange was initiated by diluting the protein to 2 μM in deuterated buffer ($pH_{measured}$ 7) at room temperature (22 ± 1 °C). Thirty microliter aliquots were taken at selected time points between 1 and 120 min and quenched to pH 2.3 using buffer acidified with formic acid (FA). These aliquots were subsequently flash frozen in liquid N_2. For spatially resolved HDX−MS experiments, the aliquots were rapidly thawed to ∼0 °C and manually injected into a nanoACQUITY UPLC with HDX technology (Waters, Milford, MA) fitted with a POROS pepsin column (2.1 mm × 30 mm) from Life Technologies/Applied Biosystems (Carlsbad, CA). Online pepsin digestion was conducted at 15 °C. Desalting and peptide separation were performed at 0 °C within 12 min on an equilibrated reversed-phase column (BEH C18, 1.7 μm particle size, 1 mm × 100 mm) using a water/acetonitrile gradient with 0.1% FA at 40 μL min^{-1}. Fully deuterated controls (m_{100}) were employed to correct for back exchange. These controls were generated by protein incubation in exchange buffer at pH 2.0 for 24 h. Samples representing the t = 0 time point yielded the corresponding m_0 values. Biolynx 4.1 and DynamX (Waters) were used for data analysis. Deuteration levels (D) were determined as

$$D\ (\%) = \left(\frac{m_t - m_0}{m_{100} - m_0}\right) \times 100\% \quad (1)$$

Experiments were performed on a Waters Synapt HDMS instrument equipped with a standard electrospray source that was operated at 2.8 kV. The source and desolvation temperatures were 80 and 300 °C, respectively, and the cone voltage was 30 V. Peptide identification was performed using tandem mass spectrometry based on the known sequences of Eε and Tε (Figure S1, Supporting Information).

Optical Measurements. CD spectra were recorded on a Jasco J-810 spectropolarimeter (Easton, MD) using a 1 mm cuvette. Blank spectra measured for protein-free solutions were subtracted from the CD data of 5 μM Tε and Eε measured in the presence and absence of 100 μM ATP. Experimental data were converted to mean residue ellipticity (θ). Analytical ultracentrifugation (AUC) experiments were performed at 20 °C on a Beckman XL-A instrument (Pasadena, CA) that was equipped with absorbance optics.[49,50] ATP-depleted Tε was dialyzed overnight against 25 mM MOPS-KOH (pH 7.0), 100 mM KCl, and 0.5 mM EDTA or the same buffer containing 25 μM ATP to allow equilibrium levels of ATP binding. These Tε samples were then analyzed by sedimentation equilibrium measurements. Samples with Tε polypeptide concentrations of 20−23 μM were loaded into cells with six-channel Epon charcoal centerpieces and a 1.2 cm path length. These samples were initially sedimented at 20 000 rpm for 20 h to allow equilibration. Absorbance measurements at 280 nm were collected in 0.002 cm radial steps and averaged over 10 scans. Comparison with scans taken 4 h earlier confirmed that equilibrium had been reached. Additional data sets were collected after subsequent equilibration at 25 000 and 30 000 rpm. All of these data were globally fit using GraphPad Prism software according to the single-species model equation

$$C = C_0 \exp\left(\frac{\omega^2}{2RT} M_{obs}(1 - \bar{v}\rho)(x^2 - x_0^2)\right) + I_0 \quad (2)$$

where C is the concentration at radius x, C_0 is the concentration at reference radius x_0, ω is the angular velocity of the rotor, $\bar{v}$ is the partial specific volume of the protein (calculated from its amino acid composition using the program SEDNTERP), ρ is the density of the solvent, R is the ideal gas constant, T is the absolute temperature, I_0 is the baseline offset, and M_{obs} is the measured molecular weight of the protein. AUC experiments conducted in the absence of KCl yielded results that were identical to those shown below within experimental error. Reported M_{obs} values represent a global fit of triplicate measurements conducted at the three rotor speeds, for a total of nine runs for each condition.

RESULTS AND DISCUSSION

Circular Dichroism. Eε exhibits a far-UV CD spectrum with a minimum around 220 nm, in accordance with earlier reports.[16] These data are consistent with a mixed helical/sheet secondary structure.[18] The addition of 100 μM ATP to Eε did not induce any significant spectral changes (Figure 2A). This finding is not surprising considering the low ATP-binding affinity of Eε[23] together with the known fact that Eε adopts a relatively well-defined structure even in the absence of ATP.[18,19] CD measurements at higher ATP concentrations were precluded by the UV absorbance of the adenine moiety. A very different behavior was observed for Tε, where the addition of 100 μM ATP induced marked alterations in the CD spectrum (Figure 2B). The data acquired for ATP-bound Tε resemble those of Eε in Figure 2A. In contrast, ATP-free Tε exhibited a less negative molar ellipticity around 222 nm, indicating a lower helicity.[51] These observations are in line with the view that Tε possesses a high ATP-binding affinity[28] and that ligand binding induces the formation of stable helical structure in the α1−α2 region.[23] One factor that promotes the high ATP affinity of Tε is the accumulation of positive charges in the binding site (mainly due to Arg residues, Figure 1D), which mediate favorable electrostatic interactions with the triphosphate group. In the case of Eε, this positive charge accumulation is less pronounced.[23] Binding of ATP^{4-} to Tε in neutral solution may also be favored by bulk electrostatics because Tε has a pI of 9.3, whereas the pI of Eε is 5.7.

dx.doi.org/10.1021/bi5004684 | Biochemistry 2014, 53, 4072−4080

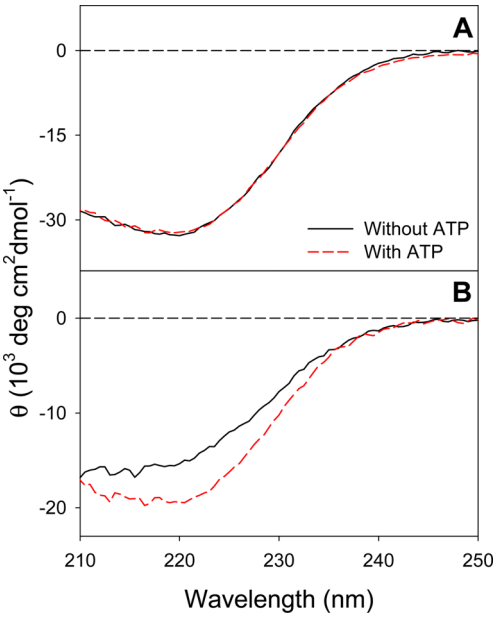

Figure 2. Far-UV CD data of (A) Eε and (B) Tε in the absence (black) and presence (red) of 100 μM ATP. All other solution additives were the same as in the subsequent HDX experiments (except for the presence of D_2O).

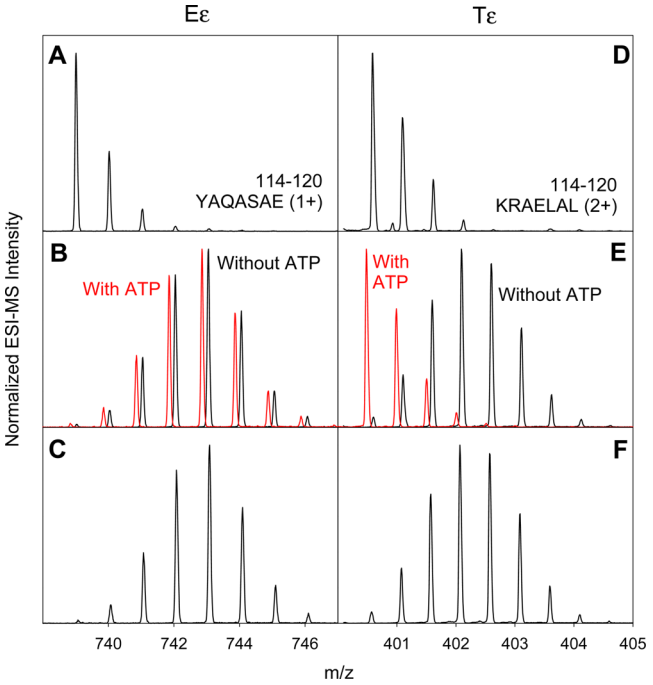

Figure 3. Unprocessed HDX–MS data for peptide 114–120 from Eε (A–C) and Tε (D–F). Spectra for unlabeled controls are shown in panels A and D. The corresponding data for the fully exchanged peptides are depicted in panels C and F. Panels B and E show data acquired in the absence (black) and in the presence (red) of ATP for a labeling time of 10 min. The latter have been shifted in this figure by −0.2 Da for better visualization.

Hydrogen/Deuterium Exchange Mass Spectrometry. Online peptic digestion of Eε and Tε yielded a large number of peptides. For each protein, 16 of these protein segments were selected that had sufficiently high S/N ratios for reliable HDX–MS measurements. The overall sequence coverage under these conditions was 99 and 86%, respectively, for Eε and Tε (Figure S1). HDX kinetics were measured with and without ATP to characterize ligand-induced changes in protein structure and dynamics. Initial experiments on Eε revealed that addition of 1 mM ATP did not cause any alterations compared to ATP-free samples (data not shown). The ATP concentration was then increased to 10 mM, which exceeds the typical intracellular value of ~3 mM.[52] However, even this elevated concentration did not induce any significant changes in the HDX behavior of Eε. As an example, unprocessed mass distributions for peptide 114–120 are depicted in Figure 3A–C. This is in contrast to the behavior of Tε, where dramatic differences in HDX kinetics were already observed after addition of 1 mM ATP (Figure 3D–F).

Deuterium uptake curves of the Eε and Tε peptides are depicted in Figures 4 and 5 (for linking residue numbers to sequence elements, see Supporting Information Figure S1). To better visualize these HDX data, the peptide-resolved deuteration levels for t = 10 min were mapped onto the crystal structures of Eε and Tε (Figure 6). It can be seen that in the absence of ATP the extent of deuteration tends to be higher for Tε than for Eε. The former shows almost complete deuteration throughout the entire protein sequence (Figure 6B), whereas Eε exhibits significant protection in the β sandwich, particularly the β8–β9 region (green, Figure 6A). Thus, in the absence of ATP, the β sandwich region is more rigid in Eε than in Tε. Helices α1 and α2 appear to be quite dynamic for both proteins under these conditions. ATP binding induces a dramatic rigidification of Tε. The largest stabilizing effects are seen for β8–β9 and α2 (blue, Figure 6C). Other Tε regions that become less dynamic upon ATP binding include parts of α1 as well as β1, β2, and β10 (green). The opposite side of the β sandwich retains high deuteration values after ATP binding (β3, β4, and β6; red/orange, Figure 6C). As noted above, no significant deuteration changes upon ATP addition are observed for Eε and therefore only a single colored panel is shown for this protein (Figure 6A).

Previous room-temperature studies on other systems indicated reduced conformational dynamics for proteins from thermophilic organisms relative to their mesophilic homologues.[53,54] Cursory comparison of Eε and Tε in the absence of ATP seems to suggest that for the two proteins examined here this trend is reversed (Figure 6A, B). However, this type of comparison does not consider the ATP-binding affinities of the two proteins, which is in the submicromolar range for Tε at room temperature,[28] whereas Eε has a K_d that is 5 orders of magnitude higher.[23] Under physiological conditions with [ATP] ≈ 3 mM,[52] this implies that Tε will predominantly exist in the ATP-bound state, whereas Eε primarily remains ligand-free. In other words, a more pertinent way to compare the physiologically relevant state of the two proteins is to contrast Eε (Figure 6A) with ATP-bound Tε (Figure 6C). From this vantage point, the mesophilic protein (Eε) is more dynamic than its thermophilic homologue (Tε) at room temperature, as previously reported for other proteins.[53,54] However, comparative analyses of the two proteins are further complicated by their different self-association propensities, as outlined in the subsequent section.

ATP-Induced Dimerization of Tε. Protein–ligand interactions often lead to greatly reduced HDX rates in the vicinity of the binding site.[55,56] On the basis of the data presented so far, the stabilization of α2 upon ATP binding to Tε (Figure 6B,C) is consistent with such a local stabilizing effect. As noted, α2 comprises two of the residues that are directly involved in

dx.doi.org/10.1021/bi5004684 | Biochemistry 2014, 53, 4072–4080

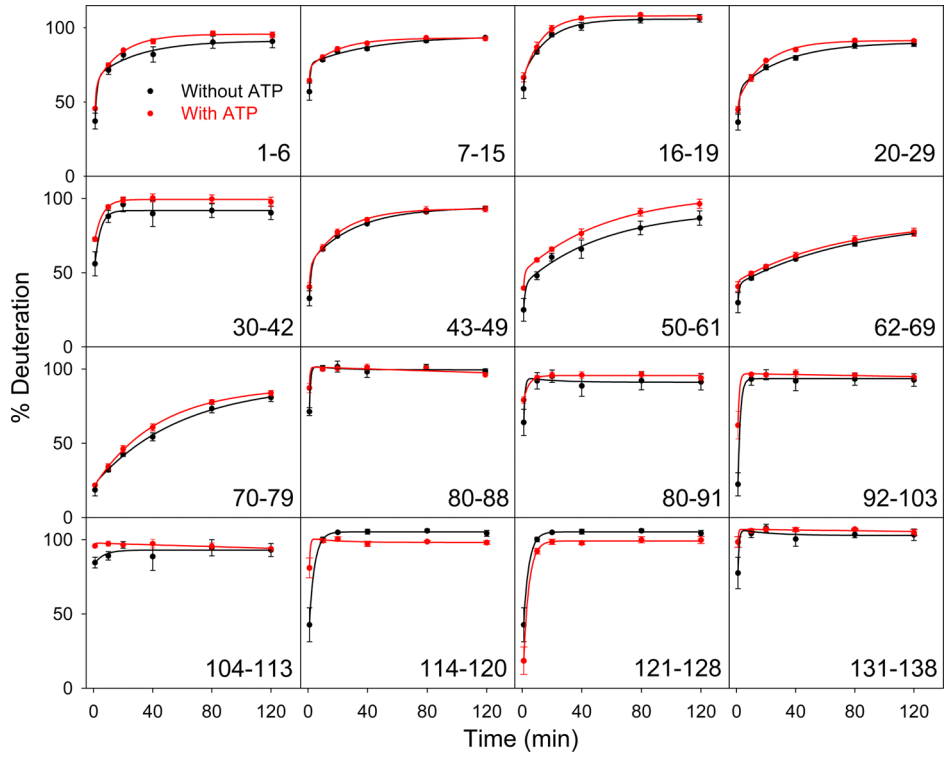

Figure 4. HDX kinetics of Eε peptides in the absence (black) and presence (red) of 10 mM ATP. Residue numbers are indicated in each panel. Lines are biexponential fits. Error bars represent standard deviations of triplicate measurements.

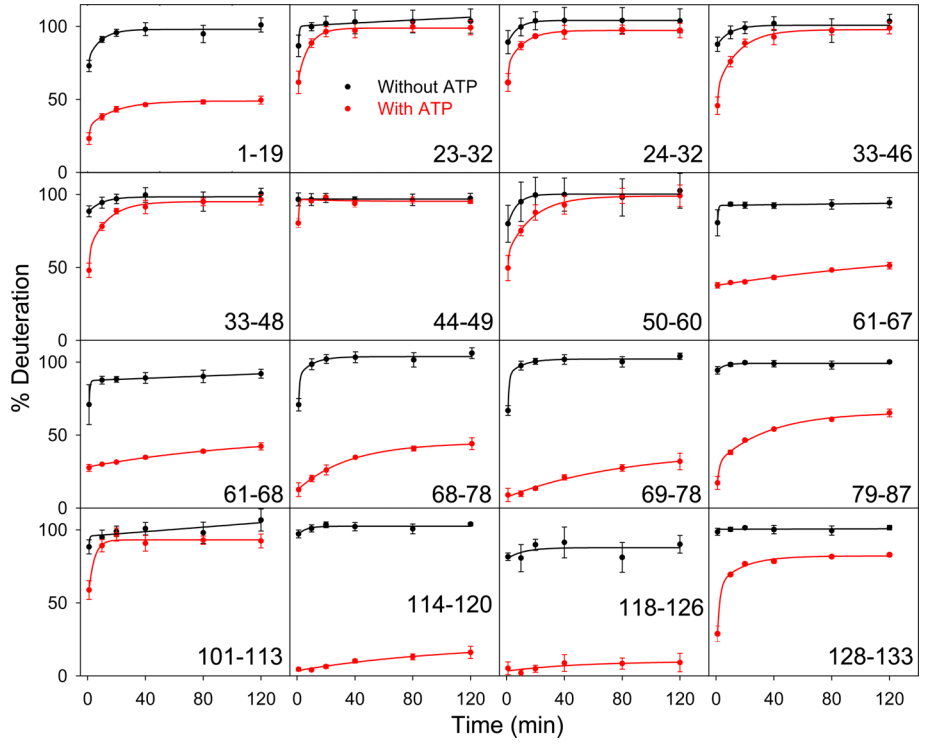

Figure 5. HDX kinetics of Tε peptides in the absence (black) and presence (red) of 1 mM ATP. For additional information, see the caption of Figure 4.

ATP binding (R122 and R126, Figure 1D). The β8−β9 segment is another area of Tε that undergoes a marked stabilization upon addition of ATP. This behavior is surprising considering that β8−β9 is quite remote from the ATP-binding site (Figure 6B,C). Allostery provides one possible explanation for such remote stabilization effects;[44,45] however, the subsequent considerations reveal that the β8−β9 protection has a different origin.

AUC experiments were conducted to gain additional insights into the properties of Tε in solution. In the absence of ATP,

dx.doi.org/10.1021/bi5004684 | *Biochemistry* 2014, 53, 4072−4080

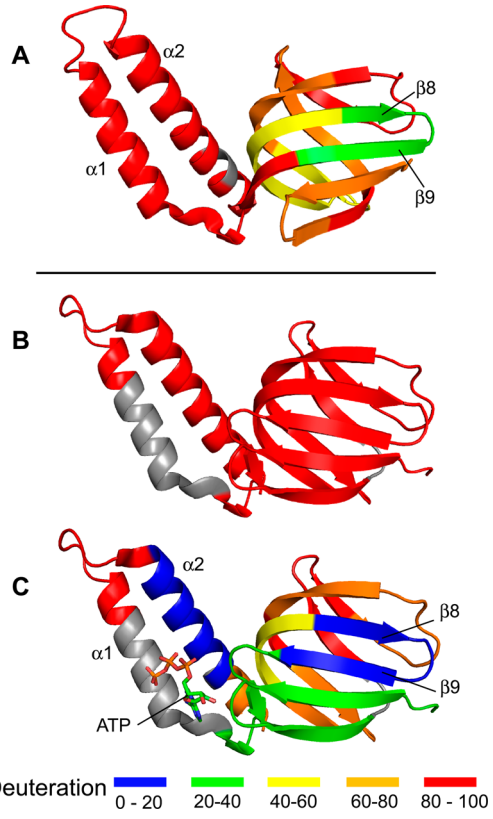

Figure 6. (A) Mapping of the t = 10 min HDX data (from Figure 4) onto the X-ray structure of Eε. (B, C) Corresponding HDX results for Tε (from Figure 5) in the absence and presence of ATP are shown in panels B and C, respectively. Colors represent deuteration percentages as defined in the legend. Gray elements denote regions for which no suitable peptides were found after peptic digestion.

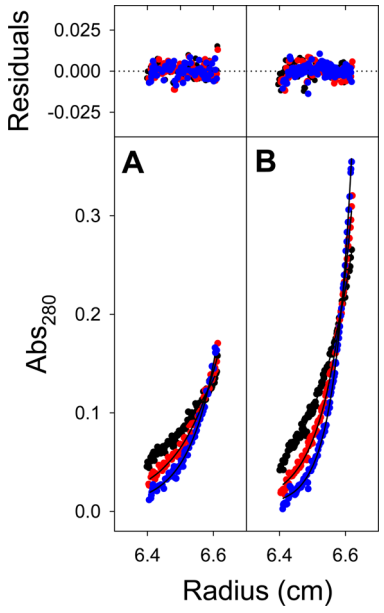

Figure 7. Sedimentation equilibrium AUC runs of Tε in the absence (A) and presence (B) of ATP measured at rotor speeds of 20 000, 25 000, and 30 000 rpm (black, red, and blue, respectively). Lines represent global fits according to eq 2.

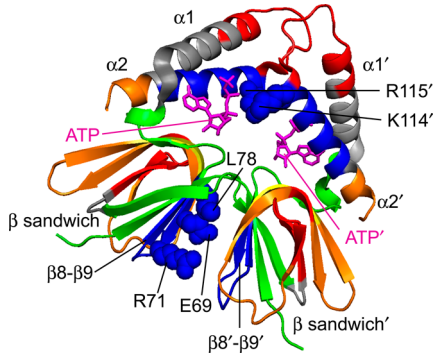

Figure 8. Crystal structure of ATP-bound dimeric Tε (PDB file 2E5Y).[23] Colors indicate deuteration percentages for t = 10 min (from Figure 6C, where blue represents the lowest deuteration levels). Selected side chains and secondary structure elements of the complex are highlighted, using the absence or presence of a prime (′) to differentiate between the two subunits. E69, R71, L78, K114, and R115 from each of the two chains form intersubunit contacts. For each of the corresponding residue pairs, only one member is highlighted to prevent cluttering.

the protein exhibits a M_{obs} value of 17.7 ± 0.4 kDa, relatively close to the 14 562 Da that is inferred from the amino acid sequence (Figure 7A). Surprisingly, addition of ATP resulted in a M_{obs} of 27.1 ± 0.2 kDa, in other words, almost twice the expected value (Figure 7B), implying that ATP-bound Tε forms a homodimer in solution. Although the M_{obs} of 27.1 kDa is too close to the expected dimer value for a precise determination of the dimerization K_d, analysis of the AUC data using a monomer−dimer model suggest it to be in the range of 3 μM.

To the best of our knowledge, the ATP-induced dimerization of Tε has not been reported before. Earlier data on the solution-phase properties of this protein were interpreted with the implicit assumption of a monomeric state.[23,28] Interestingly, X-ray crystallography provides direct evidence for the dimerization propensity of ATP-bound Tε. PDB file 2E5Y[23] shows the protein as a symmetric dimer, with one bound ATP molecule per subunit (Figure 8). Close interactions between the two chains exist in the β sandwich regions, particularly β8−β9 and β8′−β9′. These interactions are mediated by electrostatic contacts between the R71/E69/R71′/E69′ side chains, which adopt a tightly packed quadrupolar pattern. In addition, L78 and L78′ are in hydrophobic contact with each other. The significant HDX protection of β8−β9 (and β8′−β9′, blue in Figure 8) strongly suggests that these interchain contacts persist for ATP-bound Tε in solution. A second set of contacts is seen in the α1−α2/α1′−α2′ region, where the triphosphate of ATP interacts electrostatically with the K114′ and R115′ side chains from the other subunit (Figure 8). These favorable intermolecular charge−charge interactions are in addition to the contacts provided by R92, R99, R122, and R126 (Figure 1D). We conclude that the low deuteration values seen for α2 (and α2′, blue in Figure 8) after ATP binding reflect the formation of both intra- and intermolecular contacts. Overall, our data demonstrate that the monomeric structure of Figure 1D does not adequately represent the ATP-bound state of Tε. Instead, the HDX protection pattern is consistent with the dimeric crystal structure of Figure 8.[23]

Readers might be surprised that the dimeric nature of ATP-bound Tε has thus far gone unrecognized, despite the fact that the protein crystallizes as a dimer. However, it can be difficult to extrapolate from the polypeptide interactions in a crystal to the properties in solution. Various algorithms have been

dx.doi.org/10.1021/bi5004684 | Biochemistry 2014, 53, 4072−4080

proposed to distinguish biologically relevant contacts in protein crystals from packing artifacts, but these approaches tend to suffer from relatively high error rates.[57−60] The close packing of polypeptide chains in a crystal necessarily generates interchain contacts that are not present in solution. An important example in this context is Eε (1AQT),[18] which exhibits a crystal packing very similar to that of ATP-bound Tε (PDB file 2E5Y).[23] Close β8−β9/β8′−β9′ contacts are seen in both cases.[18] Despite their similar X-ray structures, Eε is monomeric in solution,[16] whereas the solution-phase state of ATP-bound Tε is a dimer (Figure 7). A difference between the β8−β9/β8′−β9′ crystal contacts for Eε and Tε is that the former primarily involve hydrophobic interactions,[18] whereas the latter have a strong electrostatic component (Figure 8). As an interesting side aspect, we note that the β8−β9 surface also mediates binding between ε and γ in intact F_1 complexes.[14,18]

CONCLUSIONS

The key finding of this work is that isolated Tε undergoes dimerization upon ATP binding. ε (or its mitochondrial homologue, δ) represents a key component of the F_0F_1 machinery. There is overwhelming evidence that ε (or δ) functions as a monomeric subunit within F_0F_1.[14,20,22] It therefore is not immediately clear if the dimerization propensity uncovered here for isolated Tε has physiological relevance. Nonetheless, the observed behavior has a number of interesting implications.

The inhibitory function of ε within F_0F_1 is linked to a conformational switch from an extended conformation to a more compact state (Figure 1A−C). In *Bacillus* PS3, this transition can be triggered by ATP binding such that Tε may serve as an ATP level sensor.[23] To obtain a better understanding of this switching event, past studies[23,28] followed an isolated-protein approach that assumed the net reaction

$$\mathrm{ATP} + \mathrm{T}\varepsilon_{\mathrm{extended}} \rightarrow \mathrm{ATP{\cdot}T}\varepsilon_{\mathrm{compact}} \quad (3)$$

It is not our intention to discredit those earlier experiments. However, the current work reveals an unexpected complication: the fact that the actual conversion exhibited by isolated Tε proceeds according to

$$2\mathrm{ATP} + 2\mathrm{T}\varepsilon_{\mathrm{extended}} \rightarrow (\mathrm{ATP{\cdot}T}\varepsilon_{\mathrm{compact}})_2 \quad (4)$$

The binding mode of ATP in the dimeric Tε complex comprises residues from both subunits, which is obviously different from the situation within F_0F_1, where only a single Tε subunit is present. In other words, mechanistic insights garnered from reaction 4 may not have direct implications for the regulatory function of Tε *in vivo*. In future work, it will be interesting to conduct a detailed investigation on the ATP-binding behavior of the Tεγ subcomplex,[61] which represents a model system that may be more physiologically relevant than isolated Tε.

The fact that eukaryotes do not use ε for regulating their F_0F_1 activity highlights the potential of ε as an antibacterial target.[14,32] The findings reported here indicate a possible drug action mechanism involving the formation of tightly bound ε dimers in the presence of a high-affinity ATP analogue. The unique nature of the I(L)DXXRA binding motif on bacterial ε[23] implies that it might be feasible to develop specific high-affinity ligands that do not interfere with the mitochondrial ATP metabolism. Intercellular sequestration of bacterial ε in a dimeric form would limit the supply of free ε that is available for the assembly of functional F_0F_1, thereby slowing the growth of the pathogen without affecting the eukaryotic host. For assessing the feasibility of such an approach, it will be necessary to conduct future studies on the ATP-binding properties and dimerization propensities of ε from a wide range of bacteria. As noted earlier, ATP−ε interactions have thus far been documented only for *Bacillus* PS3 and *E. coli*[23] as well as for *B. subtilis*.[29] It will be interesting to see if this list can be extended to other bacterial species.

ASSOCIATED CONTENT

Supporting Information

Sequences of Eε and Tε. This material is available free of charge via the Internet at http://pubs.acs.org.

AUTHOR INFORMATION

Corresponding Authors

*(S.D.D.) Telephone: (519) 661-2111 ext. 83055. E-mail: sdunn@uwo.ca.

*(L.K.) Telephone: (519) 661-2111 ext. 86313. E-mail: konerman@uwo.ca.

Funding

This work was supported by the Natural Sciences and Engineering Council of Canada (L.K.), the Canada Research Chairs Program (L.K.), and the Canadian Institutes of Health Research (FRN 10237, S.D.D.).

Notes

The authors declare no competing financial interest.

ACKNOWLEDGMENTS

All optical experiments were conducted in the UWO Biomolecular Interactions & Conformations Facility (BICF). We thank Lee-Ann Briere, manager of the BICF, for collecting and analyzing the AUC data in Figure 7 and for help with the CD measurements. We also thank Yumin Bi for her excellent technical assistance in the preparation of proteins used in these studies.

ABBREVIATIONS USED

ADP, adenosine diphosphate; ATP, adenosine triphosphate; AUC, analytical ultracentrifugation; Eε, ε subunit from *E. coli*; F_0F_1, F_0F_1-ATP synthase; HDX, hydrogen/deuterium exchange; MS, mass spectrometry; P_i, inorganic phosphate; Tε, ε subunit from *Bacillus PS3*

REFERENCES

(1) Boyer, P. D. (1997) The ATP synthase − a splendid molecular machine. *Annu. Rev. Biochem. 66*, 717−749.

(2) Stock, D., Leslie, A. G. W., and Walker, J. E. (1999) Molecular architecture of the rotary motor in ATP synthase. *Science 286*, 1700−1705.

(3) Borsch, M., and Duncan, T. M. (2013) Spotlighting motors and controls of single F_0F_1-ATP synthase. *Biochem. Soc. Trans. 41*, 1219−1226.

(4) Schmidt, C., Zhou, M., Marriot, H., Morgner, N., Politis, A., and Robinson, C. V. (2013) Comparative cross-linking and mass spectrometry of an intact F-type ATPase suggest a role for phosphorylation. *Nat. Commun. 4*, 1−11.

(5) Junge, W., Sielaff, H., and Engelbrecht, S. (2009) Torque generation and elastic power transmission in the rotary F_0F_1-ATPase. *Nature 459*, 364−370.

(6) Wachter, A., Bi, Y. M., Dunn, S. D., Cain, B. D., Sielaff, H., Wintermann, F., Engelbrecht, S., and Junge, W. (2011) Two rotary

motors in F-ATP synthase are elastically coupled by a flexible rotor and a stiff stator stalk. *Proc. Natl. Acad. Sci. U.S.A. 108*, 3924−3929.
(7) Feniouk, B. A., and Junge, W. (2005) Regulation of the F_0F_1-ATP synthase: the conformation of subunit ε might e determined by directionality of subunit γ rotation. *FEBS Lett. 579*, 5114−5118.
(8) Feniouk, B. A., Kato-Yamada, Y., Yoshida, M., and Suzuki, T. (2010) Conformational transitions of subunit ε in ATP synthase from thermophilic *Bacillus* PS3. *Biophys. J. 98*, 434−442.
(9) Shah, N. B., Hutcheon, M. L., Haarer, B. K., and Duncan, T. M. (2013) The ε-inhibited state forms after ATP hydrolysis, is distinct fom the ADP-inhibited state, and responds dnamically to catalytic site ligands. *J. Biol. Chem. 288*, 9383−9395.
(10) Hirono-Hara, Y., Noji, H., Nishiura, M., Muneyuki, E., Hara, K. Y., Yasuda, R., Kinosita, K., and Yoshida, M. (2001) Pause and rotation of F-1-ATPase during catalysis. *Proc. Natl. Acad. Sci. U.S.A. 98*, 13649−13654.
(11) Saita, E., Iino, R., Suzuki, T., Feniouk, B. A., Kinosita, K., and Yoshida, M. (2010) Activation and stiffness of the inhibited states of F-1-ATPase probed by single-molecule manipulation. *J. Biol. Chem. 285*, 11411−11417.
(12) Bulygin, V. V., Duncan, T. M., and Cross, R. L. (1998) Rotation of the epsilon subunit during catalysis by *Escherichia coli* F_0F_1-ATP synthase. *J. Biol. Chem. 273*, 31765−31769.
(13) Kato-Yamada, Y., Noji, H., Yasuda, R., Kinosita, K., and Yoshida, M. (1998) Direct observation of the rotation of epsilon subunit in F-1-ATPase. *J. Biol. Chem. 273*, 19375−19377.
(14) Cingolani, G., and Duncan, T. M. (2011) Structure of the ATP synthase catalytic complex (F_1) from *Escherichia coli* in an auto-inhibited conformation. *Nat. Struct. Mol. Biol. 18*, 701−708.
(15) Cipriano, D. J., and Dunn, S. D. (2006) The role of the ε subunit in the *Escherichia coli* ATP Synthase: the C-terminal domain is required for efficient energy coupling. *J. Biol. Chem. 281*, 501−507.
(16) Sternweis, P. C., and Smith, J. B. (1980) Characterization of the inhibitory (epsilon) subunit of the proton-translocating adenosine triphosphatase from *Escherichia coli*. *Biochemistry 19*, 526−531.
(17) Dunn, S. D., Tozer, R. G., and Zadorozny, V. D. (1990) Activation of *Escherichia coli* F1 ATPase by lauryldimethylamine oxide and ethylene glycol: relationship of ATPase activity to the interaction of the epsilon and beta subunits. *Biochemistry 29*, 4335−4340.
(18) Uhlin, U., Cox, G. B., and Guss, J. M. (1997) Crystal structure of the ε subunit of the proton-translocating ATP synthase from *Escherichia coli*. *Structure 5*, 1219−1230.
(19) Wilkens, S., and Capaldi, R. A. (1998) Solution structure of the epsilon subunit of the F-1-ATPase from *Escherichia coli* and interactions of this subunit with beta subunits in the complex. *J. Biol. Chem. 273*, 26645−26651.
(20) Gibbons, C., Montgomery, M. G., Leslie, A. G. W., and Walker, J. E. (2000) The structure of the central stalk in bovine F-1-ATPase at 2.4 angstrom resolution. *Nat. Struct. Biol. 7*, 1055−1061.
(21) Dallmann, H. G., Flynn, T. G., and Dunn, S. D. (1992) Determination of the 1-ethyl-3-(3-dimethylamino)propyl-carbodiimide-induced cross-link between the beta and epsilon subunits of *Escherichia coli* F1-ATPase. *J. Biol. Chem. 267*, 18953−18960.
(22) Rodgers, A. J. W., and Wilce, M. C. J. (2000) Structure of the gamma-epsilon complex of ATP synthase. *Nat. Struct. Biol. 7*, 1051−1054.
(23) Yagi, H., Kajiwara, N., Tanaka, H., Tsukihara, T., Kato-Yamada, Y., Yoshida, M., and Akutsu, H. (2007) Structures of the thermophilic F_1-ATPase ε subunit suggesting ATP-regulated arm motion of its C-terminal domain in F_1. *Proc. Natl. Acad. Sci. U.S.A. 104*, 11233−11238.
(24) Tsunoda, S. P., Rodgers, A. J. W., Aggeler, R., Wilce, M. C., Yoshida, M., and Capaldi, R. A. (2001) Large conformational changes of the ε subunit in the bacterial F_1F_0 ATP synthase provide a ratchet action to regulate this rotary motor enzyme. *Proc. Natl. Acad. Sci. U.S.A. 98*, 6560−6564.
(25) Suzuki, A., Murakami, K., Lino, R., Suzuki, J., Ono, S., Shirakihara, Y., and Yoshida, M. (2003) F_0F_1-ATPase/synthase is geared to the synthesis mode by conformational rearrangement of ε subunit in response to proton motive force and ADP/ATP balance. *J. Biol. Chem. 278*, 46840−46846.
(26) Kato-Yamada, Y., and Yoshida, M. (2003) Isolated ε subunit of thermophilic F_1-ATPase binds ATP. *J. Biol. Chem. 278*, 36013−36016.
(27) Kadoya, F., Kato, S., Watanabe, K., and Kato-Yamada, Y. (2011) ATP binding to the ε subunit of thermophilic ATP synthase is crucial for efficient coupling of ATPase and H^+ pump activities. *Biochem. J. 437*, 135−140.
(28) Iino, R., Murakami, T., Iizuka, S., Kato-Yamada, Y., Suzuki, T., and Yoshida, M. (2005) Real-time monitoring of conformational dynamics of the ε subunit in F_1-ATPase. *J. Biol. Chem. 280*, 40130−40134.
(29) Kato-Yamada, Y. (2005) Isolated ε subunit of *Bacillus subtilis* F_1-ATPase binds ATP. *FEBS Lett. 579*, 6875−6878.
(30) Yagi, H., Konno, H., Murakami-Fuse, T., Isu, A., Oroguchi, T., and Akutsu, H. (2010) Structural and functional analysis of the intrinsic inhibitor subunit ε of F_1-ATPase from photosynthetic organisms. *Biochem. J. 425*, 85−94.
(31) Campanella, M., Parker, N., Tan, C. H., Hall, A. M., and Duchen, M. R. (2009) IF1: setting the pace of the F_1F_0-ATP synthase. *Trends Biochem. Sci. 34*, 343−350.
(32) Andries, K., Verhasselt, P., Guillemont, J., Gohlmann, H. W. H., Neefs, J. M., Winkler, H., Van Gestel, J., Timmerman, P., Zhu, M., Lee, E., Williams, P., de Chaffoy, D., Huitric, E., Hoffner, S., Cambau, E., Truffot-Pernot, C., Lounis, N., and Jarlier, V. (2005) A diarylquinoline drug active on the ATP synthase of *Mycobacterium tuberculosis*. *Science 307*, 223−227.
(33) Konermann, L., Pan, J., and Liu, Y. (2011) Hydrogen exchange mass spectrometry for studying protein structure and dynamics. *Chem. Soc. Rev. 40*, 1224−1234.
(34) Kaltashov, I. A., Bobst, C. E., and Abzalimov, R. R. (2013) Mass spectrometry-based methods to study protein architecture and dynamics. *Protein Sci. 22*, 530−544.
(35) Iacob, R. E., and Engen, J. R. (2012) Hydrogen exchange mass spectrometry: are we out of the quicksand? *J. Am. Soc. Mass Spectrom. 23*, 1003−1010.
(36) Englander, S. W. (2006) Hydrogen exchange and mass spectrometry: a historical perspective. *J. Am. Soc. Mass Spectrom. 17*, 1481−1489.
(37) Rob, T., Liuni, P., Gill, P. K., Zhu, S. L., Balachandran, N., Berti, P. J., and Wilson, D. J. (2012) Measuring dynamics in weakly structured regions of proteins using microfluidics-enabled subsecond H/D exchange mass spectrometry. *Anal. Chem. 84*, 3771−3779.
(38) Johnson, R. S., and Walsh, K. A. (1994) Mass spectrometric measurement of protein amide hydrogen exchange rates of apo- and holo-myoglobin. *Protein Sci. 3*, 2411−2418.
(39) Powell, K. D., Ghaemmaghami, S., Wang, M. Z., Ma, L., Oas, T. G., and Fitzgerald, M. C. (2002) A general mass spectrometry-based assay for the quantitation of protein-ligand binding interactions in solution. *J. Am. Chem. Soc. 124*, 10256−10257.
(40) Zhu, M. M., Rempel, D. L., Du, Z. H., and Gross, M. L. (2003) Quantification of protein-ligand interactions by mass spectrometry, titration, and H/D exchange: PLIMSTEX. *J. Am. Chem. Soc. 125*, 5252−5253.
(41) Asuru, A. P., An, M., and Busenlehner, L. S. (2012) Dissection of porphyrin-induced conformational dynamics in the heme biosynthesis enzyme ferrochelatase. *Biochemistry 51*, 7116−7127.
(42) Keppel, T. R., Howard, B. A., and Weis, D. D. (2011) Mapping unstructured regions and synergistic folding in intrinsically disordered proteins with amide H/D exchange mass spectrometry. *Biochemistry 50*, 8722−8732.
(43) Bai, Y., Milne, J. S., Mayne, L., and Englander, S. W. (1993) Primary structure effects on peptide group hydrogen exchange. *Proteins: Struct., Funct., Genet. 17*, 75−86.
(44) Percy, A. J., Rey, M., Burns, K. M., and Schriemer, D. C. (2012) Probing protein interactions with hydrogen/deuterium exchange and mass spectrometry − a review. *Anal. Chim. Acta 721*, 7−21.
(45) Chalmers, M. J., Busby, S. A., Pascal, B. D., West, G. M., and Griffin, P. R. (2011) Differential hydrogen/deuterium exchange mass

spectrometry analysis of protein−ligand interactions. *Exp. Rev. Proteomics 8*, 43−59.
(46) Skakoon, E. N., and Dunn, S. D. (1993) Location of conserved residue histidine-38 of the ε subunit of *Escherichia coli* ATP synthase. *Arch. Biochem. Biophys. 302*, 272−278.
(47) Cipriano, D. J., and Dunn, S. D. (2002) Genetic fusions of globular proteins to the ε subunit of the *Escherichia coli* ATP synthase. *J. Biol. Chem. 277*, 16782−16790.
(48) Hara, K. Y., Kato-Yamada, Y., Kikuchi, Y., Hisabori, T., and Yoshida, M. (2001) The role of the βDELSEED motif of F_1-ATPase. *J. Biol. Chem. 276*, 23969−23973.
(49) Schuck, P. (2000) Size-distrubution analysis of macromolecules by sedimentation velocity ultracentrifugation and Lamm equation modeling. *Biophys. J. 3*, 1606−1619.
(50) Schuck, P., Perugini, M. A., Gonzales, N. R., Howlett, G. J., and Schubert, D. (2002) Size-distrubution analysis of proteins by analytical ultracentrifugation: strategies and application to model systems. *Biophys. J. 82*, 1096−1111.
(51) Kelly, S. W., Jess, T. J., and Price, N. C. (2005) How to study protein by circular dichroism. *Biochim. Biophys. Acta 1751*, 119−139.
(52) Schneider, D. A., and Gourse, R. L. (2004) Relationship between growth rate and ATP concentration in *Escherichia col*i − a bioassay for available cellular ATP. *J. Biol. Chem. 279*, 8262−8268.
(53) Liang, Z.-X., Lee, T., Resing, K. A., Ahn, N. G., and Klinman, J. P. (2004) Thermal-activated protein mobility and its correlation with catalysis in thermophilic alcohol dehydrogenase. *Proc. Natl. Acad. Sci. U.S.A. 101*, 9556−9561.
(54) Wolf-Watz, M., Thai, V., Henzler-Wildman, K., Hadjipavlou, G., Eisenmesser, E. Z., and Kern, D. (2004) Linkage between dynamics and catalysis in a thermophilic-mesophilic enzyme pair. *Nat. Struct. Mol. Biol. 11*, 945−949.
(55) Sperry, J. B., Smith, C. L., Caparon, M. G., Ellenberger, T., and Gross, M. L. (2011) Mapping the protein−protein interface between a toxin and its cognate antitoxin from the bacterial pathogen *Streptococcus pyogenes*. *Biochemistry 50*, 4038−4045.
(56) Nakazawa, S., Hashii, N., Harazono, A., and Kawasaki, N. (2012) Analysis of oligomeric stability of insulin analogs using hydrogen/deuterium exchange mass spectrometry. *Anal. Biochem. 420*, 61−67.
(57) Sardis, M. F., and Economou, A. (2010) SecA: a tale of two protomers. *Mol. Microbiol. 76*, 1070−1081.
(58) Carugo, O., and Argos, P. (1997) Protein−protein crystal-packing contacts. *Protein Sci. 6*, 2261−2263.
(59) Xu, Q. F., Canutescu, A. A., Wang, G. L., Shapovalov, M., Obradovic, Z., and Dunbrack, R. L. (2008) Statistical analysis of interface similarity in crystals of homologous proteins. *J. Mol. Biol. 381*, 487−507.
(60) Krissinel, E., and Henrick, K. (2007) Inference of macro-molecular assemblies from crystalline state. *J. Mol. Biol. 372*, 774−797.
(61) Iizuka, S., Kato, S., Yoshida, M., and Kato-Yamada, Y. (2006) γε sub-complex of thermophilic ATP synthase has the ability to bind ATP. *Biochem. Biophys. Res. Commun. 349*, 1368−1371.